# Onset of rebound suppression in non-Newtonian droplets post-impact on superhydrophobic surfaces

Purbarun Dhar,* Soumya Ranjan Mishra, and Devranjan Samanta†
*Department of Mechanical Engineering, Indian Institute of Technology Ropar, Rupnagar–140001, India*

(Received 4 April 2019; published 22 October 2019)

Droplet deposition after impact on superhydrophobic surfaces has been an important area of study in recent years for its potential application in reduction of pesticides usage. Minute numbers of long-chain polymers added to water have been known to arrest the droplet rebound effect on superhydrophobic surfaces. Previous studies have attributed different reasons like extensional viscosity, dominance of elastic stresses, or slowing down of the contact line in the retraction phase due to stretching of polymer chains. The present study attempts to unravel the existence of critical criteria of polymer concentration and impact velocity on the inhibition of droplet rebound. The impact velocity will indirectly influence the shear rate during the retraction phase, and the polymer concentration dictates the relaxation timescale of the elastic fluids. Finally, we show that the governing Weissenberg number (at onset of retraction), which quantifies both the elastic effects of polymer chains and the hydrodynamics, is the critical parameter in determining the regime of onset of rebound suppression, and that there is a critical value which determines the onset of bounce arrest. The previous three causes, which are manifestations of elastic effects in non-Newtonian fluids, can be related to the proposed Weissenberg number criterion.

DOI: 10.1103/PhysRevFluids.4.103303

## I. INTRODUCTION

Research on impact dynamics of non-Newtonian droplets has garnered momentum since the seminal paper by Bergeron *et al.* [1]. Addition of minute amounts of flexible polymers in Newtonian base fluid without significant change in viscosity causes suppression of droplet rebound after impact on superhydrophobic (SH) surfaces. Initially, it was proposed that the high elongational viscosity of non-Newtonian fluids decelerates the retraction velocity of the droplet after the impact, which suppresses the rebound phase. However, the role of extensional viscosity was ruled out, as it will affect both spreading and retraction phases, whereas experimental observations show that only retraction behavior is changed due to polymer effects [2,3]. Subsequently, Bonn *et al.* [4] proposed the dominant role of elastic normal stresses over the surface tension, which is the driving force for drop retraction. Another study [5] proposed that the contact line is slowed down during retraction due to the stretching of the flexible polymer chains near the droplet edge.

Suppression of droplet rebound on hydrophobic surfaces has potential applications in reduction of pesticides during spraying and reducing environmental damage due to ground contamination of pesticides [1]. Other industrial applications like inkjet printing, slot coating [6], spray coating, and cooling [7] may be improved from the studies of non-Newtonian droplet impact dynamics. Droplet rebound suppression is also achieved by addition of specific surfactants [8], although

*purbarun@iitrpr.ac.in, purbarun.iit@gmail.com
†Corresponding author: devranjan.samanta@iitrpr.ac.in

 

generation of smaller droplets and splashing is not always inhibited. Application of electric field on nonaxisymmetric droplets was also found effective towards inhibiting droplet rebound [9,10]. Some other studies have focused on spreading and splashing behavior of droplets of yield stress fluids and shear thickening nature due to modulation in microstructures of hydrophobic surfaces [11–13]. For shear thickening fluid, irrespective of impact velocity, the droplet freezes into a deformed state while spreading, thereby arresting all subsequent dynamics like fragmentation or rebound typical of Newtonian fluid droplets.

Earlier works [1,4,5] may inadvertently generate an impression that any amount of polymer or impact velocity will cause the droplet to stick to the hydrophobic surface during retraction. The present paper aims to highlight the role of critical polymer concentration and impact velocity on the onset of droplet rebound suppression for non-Newtonian droplets. We hypothesize that the onset of inhibition of the rebound depends on the relaxation time (manifested through the polymer concentration in water) and the shear rate at the contact line during the retraction phase. We will present the potential role of the Weissenberg number in governing the droplet rebound inhibition. The role of extensional viscosity on the longevity of the thin filaments formed during droplet rebound process is also highlighted.

## II. EXPERIMENTAL DETAILS

Figure 1 shows the experimental setup used in our studies. Experiments were performed with a digitized precision droplet dispenser setup [14]. Impact velocity of the droplets was changed by changing the height of discharge (from a microliter syringe). The superhydrophobic (SH) surfaces were made by spray coating with a commercial liquid repellent (Ultratech Ever-Dry, USA). The surfaces prepared exhibit static contact angles of $\sim 152^\circ$ for water droplets, and a roll-off angle of $\sim 3-4^\circ$. Aqueous solutions of polyacrylamide (PAAM, Sigma Aldrich) ($\sim$5 million molecular weight) of different concentrations were used as working fluids. Homogeneous solutions were prepared using a magnetic stirrer for 2 h. Image acquisition was done with a high-speed camera (FastCam SA4, Photron) at 3600 fps. Rheological parameters like shear viscosity, viscoelastic moduli, and relaxation time were measured with a rotational rheometer (Anton Paar) with parallel plate geometry.

Surface tension of the liquids was determined by the pendant drop method. Minimal changes in the surface tension were noted (within $\pm 3\% - 5\%$ of the surface tension of water). The static contact angles were determined from image analysis, and no appreciable change in the wetting state due to addition of polymer is noted (the change in the static contact angle was within $5^\circ - 7^\circ$ compared to the water droplet). The contact angle hysteresis was also measured by the standard advancing and receding contact angle method. The contact angle hysteresis was noted to be $\sim 3^\circ$ and $\sim 5^\circ$ for water and 1500 ppm PAAM solution droplets. The droplet diameters are of 2.7–2.9 mm and the impact Weber number ranges from 50 to 250, which is of the same order of magnitude reported in previous study (Bonn *et al.* [4]).

## III. RESULTS AND DISCUSSION

We start with the case where droplet rebound is suppressed. Figure 2 shows the spatiotemporal evolution of a 1500 ppm PAAM solution droplet on a SH surface. Figure 2(a) shows the maximum spreading of the diameter after impact. During retraction [Figs. 2(c)–2(f)], the droplet gets attached to one location, exhibiting thin filament formation at the ground and a mushroom-like cloud structure at the top. The thin filament has a short lifetime ($\sim$few milliseconds) before the mushroom-like structure eventually settles down to the ground due to gravity [Figs. 2(g) and 2(h)]. Rheological measurements reveal that the dilute PAAM solutions exhibit augmented elastic moduli with negligible increase in the shear viscosity (typically Boger fluids). The transient thin filament formation is observed due to the viscoelastic nature of the fluids.

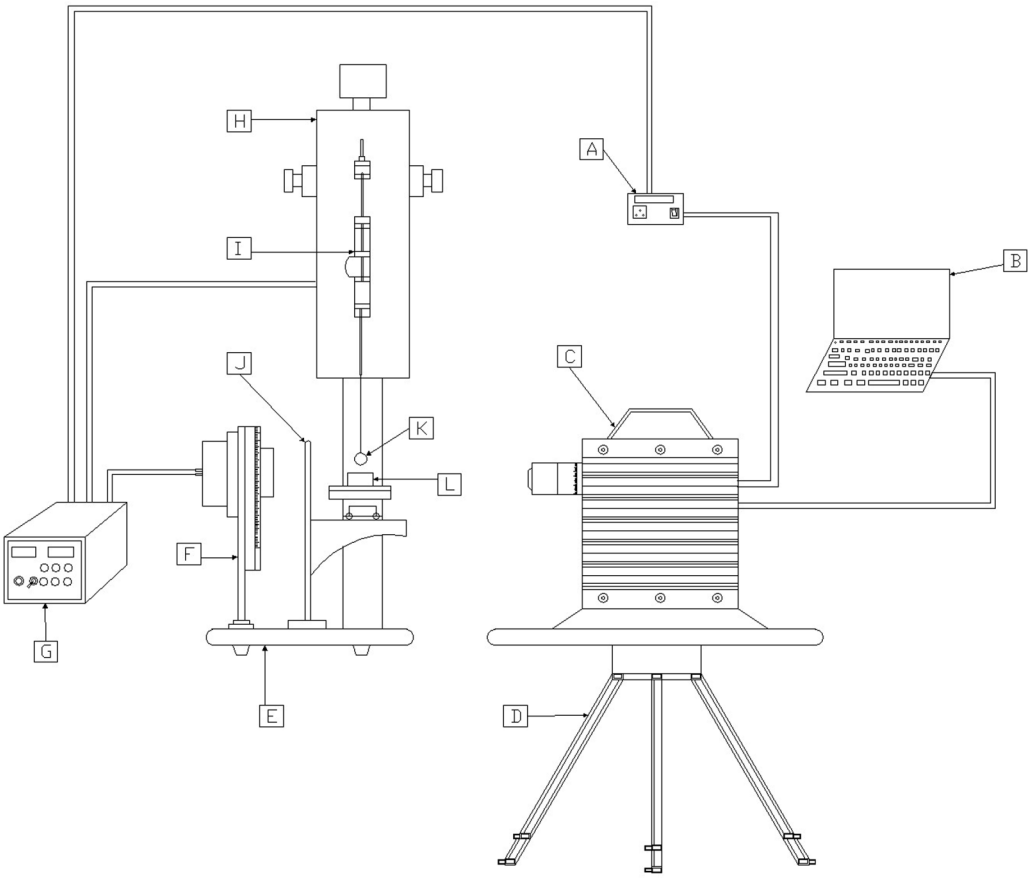


FIG. 1. Schematic of the experimental setup: (A) power supply, (B) laptop, (C) high-speed camera, (D) tripod, (E) base, (F) back light arrangement, (G) drop dispenser controller, (H) dispenser, (I) syringe holder, (J) substrate holder (clamp), (K) pendant droplet, and (L) substrate inclination apparatus.

### A. Role of polymer concentration

Subsequently, we studied the role of polymer concentration on the droplet rebound dynamics at a fixed velocity (refer to Fig. 3). We have fixed the impact velocity at 2.25 m/s for different polymer concentrations. For low polymer concentrations (50 ppm), droplets rebound like Newtonian cases,

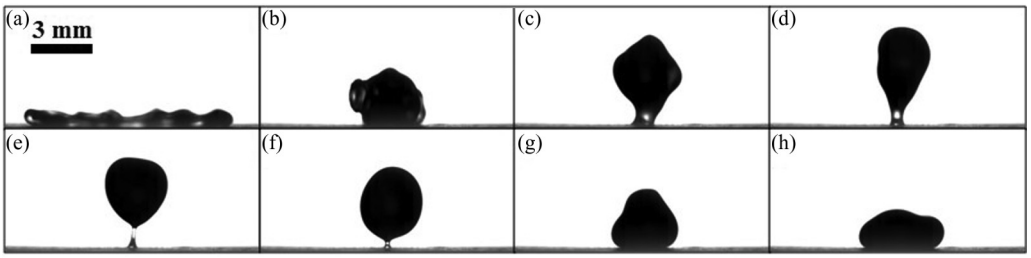


FIG. 2. Evolution of a droplet of 1500 ppm aqueous PAAM solution post-impact on a SH surface, with an impact velocity of 2.25 m/s. The images are temporally spaced 5.56 ms apart.

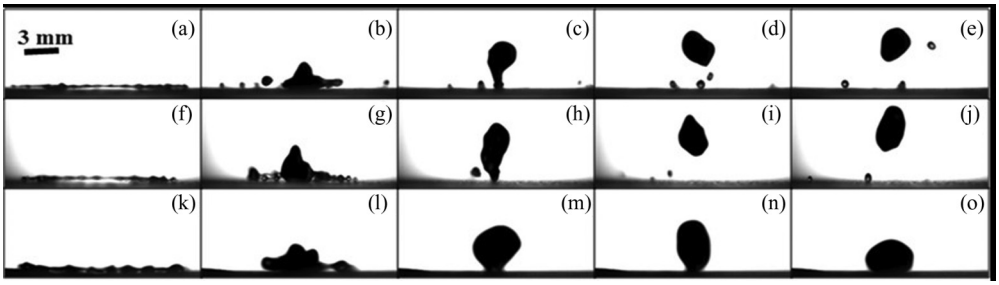


FIG. 3. Influence of polymer concentration: (a)–(e) 50 ppm; (f)–(j) 200 ppm; (k)–(o) 500 ppm PAAM solution droplet impact dynamics on SH surface with an impact velocity of 2.25 m/s. The images are temporally spaced by a time interval of 6.95 ms. Panels (e) and (j) do not represent the highest height achieved after the rebound.

albeit with a lower degree of fragmentation. Even a very short-lived filament formation was noticed for both 50 ppm [Fig. 3(c)] and 200 ppm [Figs. 3(h) and 4 row (iii)]. As we increase the polymer concentration, the filament survives long enough to allow the gravitational settling down of the top heavier portion, thereby arresting the droplet rebound off the surface. In our studies, droplet rebound is achieved with a critical polymer concentration of approximately 500 ppm. However, this is true only for impact velocities of 2.25 m/s and above.

In addition, reduced fragmentation into secondary droplets was observed for 50 and 200 ppm (refer to Fig. 4). Reduced fragmentation was reported earlier in cases of polymeric jets [15,16]. With increasing polymer concentration, thin filaments were formed at the droplet rim during retraction, leading to the generation of a lower number of secondary smaller droplets. Also, detachment of the secondary droplets was arrested, and the filaments recoiled to retract the secondary droplets to fuse with the mother droplet. Top views of drop impact dynamics of water and aqueous solutions of PAAM (100 and 200 ppm) are presented for qualitative comparison in Fig. 4. For the same time

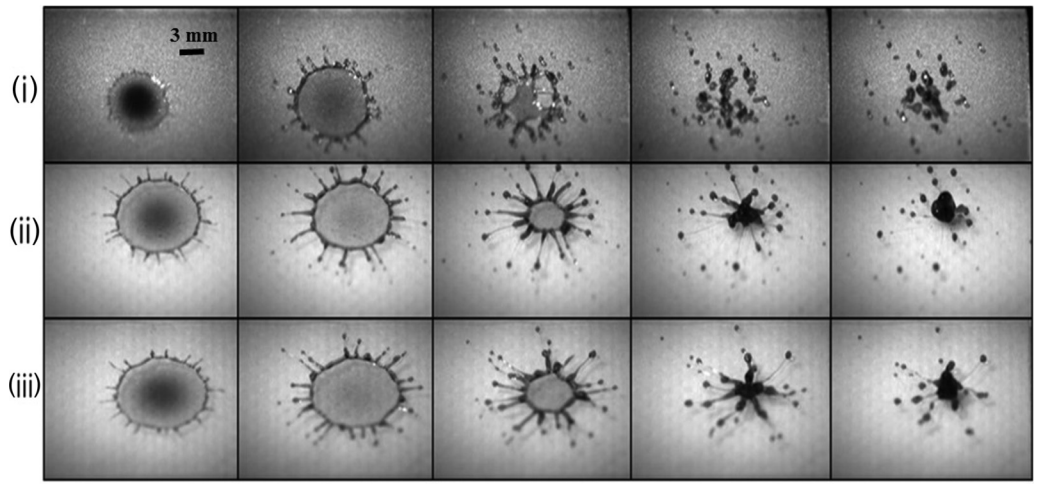


FIG. 4. Top view images for (i) water, (ii) 100 ppm, and (iii) 200 ppm PAAM droplets with an impact velocity of 2.25 m/s; addition of polymer showing the inhibition of fragmentation of smaller droplets and enhancement of filaments formed during retraction phase. A clear indication of the role of the elastic nature of the fluid can be noted by comparing the pictures in the third column of each row. Images of each row are 2.16 ms apart.

interval, it can be readily observed that the thin filaments formed during splashing are intact in case of the non-Newtonian fluids, whereas the water droplet exhibits fragmentation into secondary droplets (which tend to scamper away from the impact spot). This accentuates the idea of adding minute amounts of such polymers to reduce pesticide and fertilizer wastage during crop spraying.

### B. Role of shear rate

Then we tried to probe the role of shear rate which also influences the viscoelastic effects and directly depends on impact velocity. The velocity at retraction is dependent on the impact kinetic energy and the surface energy due to the interaction of the fluid with the surface. During the spreading regime on the superhydrophobic surfaces, the loss of initial energy due to viscous resistance at the solid-liquid interface is minimal as wetting state is not achieved while spreading. Thereby, the net energy available at the recoil phase is higher for such droplets, as is evident from the bouncing. Thereby a droplet impacting at higher kinetic energy will have higher retraction velocity and consequently shear rates at retraction (unless fragmentation or splash-aided loss of energy occurs).

Viscoelastic effects due to stretching and coiling of polymer chains become more prominent at higher shear rates. Higher shear rates (at the moment of retraction) are achieved with higher velocities at the moment of impact. Even for the highest polymer concentration tested, there is a certain critical velocity below which the shear rates are not strong enough to induce viscoelastic effects for suppressing the droplet rebound. This is analogous to a polymer-induced drag reduction scenario where no change in drag behavior is observed in laminar flow since the shear force in the flow field is not enough to stretch polymer chains to an extent which can induce elastic effects [17]. Keeping the polymer concentration constant at 1500 ppm, we varied the impact velocity in the experiments. Figure 5 shows the effect of impact velocity (and hence shear rates) on the droplet rebound.

At the lowest velocity [Fig. 5 row (i)], the droplet rebounds without a trace of filament formation. With increased velocity [Fig. 5 row (ii), (c)–(f)], filament formation is observed both at the ground and between the two parts of the drop. The subsequent shapes resemble bowling pins [Fig. 5 row (ii), (c)], or mushrooms or balloons [Fig. 5 row (ii), (e) or (f)] or wine glasses [Fig. 5 row (iii), (e), and (iv), (e)]. Such droplet shapes are never achieved with Newtonian fluids. With increasing velocity, droplet rebound suppression occurs quicker within the timeframe presented in this figure [Fig. 5 row (iv)]. Filament dynamics was observed but no bead formation/blistering were apparent, possibly due to lower strain rates unlike pure extensional rheological flows of non-Newtonian fluids [15,18–20].

The longevity of the filaments formed at the base [Fig. 5 row (iv)] during retraction of 1500 ppm PAAM solution has been provided in the Supplemental Material (Fig. SI 1, with corresponding discussion [21]). The pinning of the filaments to the substrate may be due to the droplet attaining the Cassie-to-Wenzel transition (CWT) state, also known as impalement [22–24], which can be verified in future work. However, it must be noted that previous studies discussing this behavior [22–24] were for water droplet impact on different hydrophobic surfaces, where a viscoelastic effect was absent in the flow dynamics. Further, these studies employed structured superhydrophobic surfaces where such transitions are plausible. The present surfaces are spray-coated unstructured surfaces where such states are not well defined. Thereby it cannot be concluded that wetting state transition is the sole reason behind droplet rebound suppression, especially in the present context where the surfaces were not structured SH surfaces.

We have done experiments on a series of the same substrate; however, water droplets are consistently noted to rebound, but polymer droplets of a fixed concentration showed suppression of rebound once the impact velocity exceeds a critical velocity. The surfaces have been characterized using optical and electron microscopy (refer Fig. SI 3 in the Supplemental Material), and the surfaces are confirmed to be unstructured superhydrophobic surfaces. Measurements show (refer to the Supplemental Material for discussion) that the nature of the surfaces will typically lead to

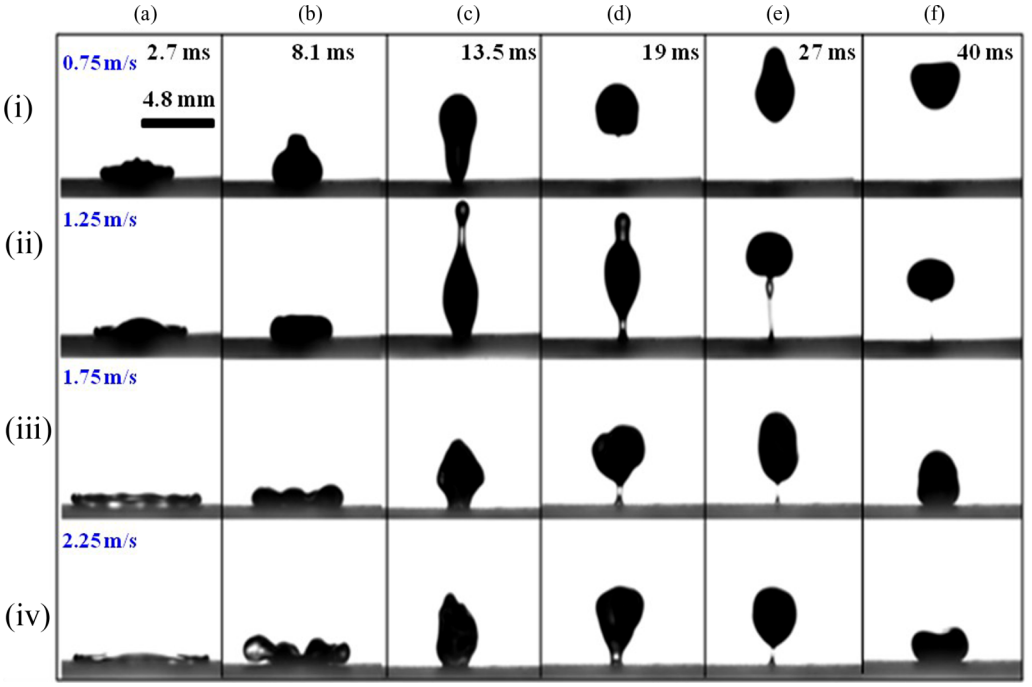


FIG. 5. Influence of impact velocity on droplet dynamics of 1500 ppm PAAM solution. Left to right shows the temporal evolution and top to bottom shows impact velocity. The propensity of rebound suppression improves with increasing impact velocity. Movies of experiments described in rows (i) and (iv) are in movie format in the Supplemental Material.

Cassie-Baxter states, which is reiterated by the very low roll-off angle. The surface does not show any structures which may induce partial or full CWT. Detailed three-dimensional, droplet impact simulations [25] show that the present surfaces have structural characteristics where the impalement of the drops during impact, and thus CWT, is not feasible. Thereby the change is wetting behavior can be ruled out as a governing mechanism for rebound suppression on the present surfaces.

Higher longevity of the thin filaments formed at the base may lead to a higher probability of droplet rebound suppression. The elastic recoil of the filaments counters the surface energy component, which promotes antiwetting (subsequent ejection off the surface). In a previous study [18] it was shown that micron-scale-thick filaments between two beads at higher concentrations (1000 ppm polyethylene oxide, PEO, which is of similar molecular weight as PAAM) never break. Likewise, in our case, the filaments connecting the surface and the upper mushroom-like portion exhibit higher lifetimes with increasing polymer concentration. Previous studies [16] suggest that the increase of polymer concentration causes enhancement of extensional viscosity, leading to enhanced stability of thin filaments formed at the base.

The role of extensional viscosity during the formation of filament pinned to the ground can be explored in future studies with capillary (extensional) rheometer facilities. Some further discussions on the nature of the filament longevity with increasing impact velocity for a given polymer concentration, and its mechanics, have been provided in the Supplemental Material (Fig. SI 1). It is worth mentioning that preliminary experiments on inclined planes showed the existence of even longer filaments (with large lifetimes) formed from the base. Although the upper heavier part is attached to the filament for a considerable time in the context of droplet impact dynamics, eventually the larger portion gets detached from the filament and rolls down along the inclined plane due to gravitational potential (refer to Fig. 6).

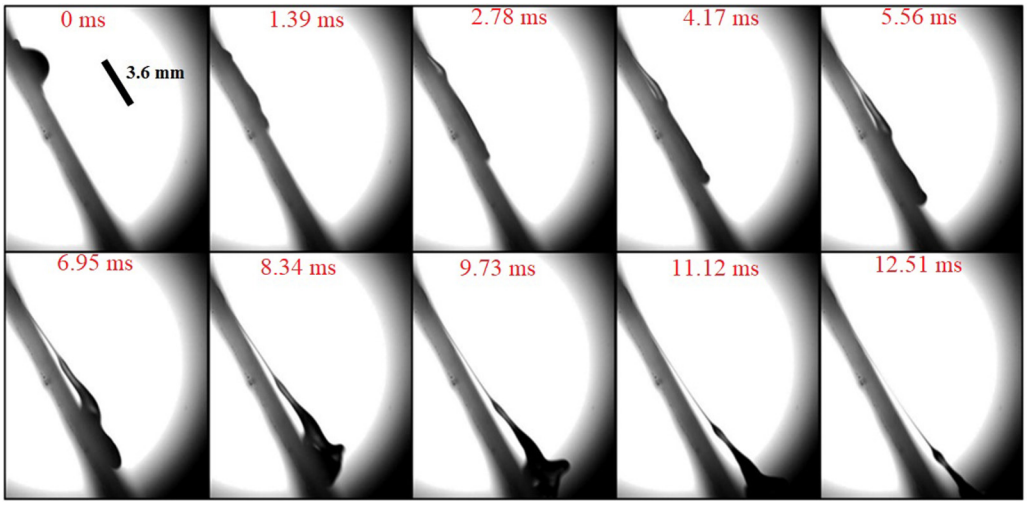


FIG. 6. Impact dynamics of 1500 ppm on an inclined SH surface at 60° w.r.t. the ground. Impact velocity is 2.25 m/s. The array highlights the role and lifetime of the filaments in case of elastic fluid impact and its subsequent role (in horizontal case) in suppressing the rebound off the surface. Images were taken at 1.39 ms intervals. The corresponding video clip is provided in the Supplemental Material.

### C. Role of Weissenberg number

Based on Figs. 2–6, it is evident that both polymer concentration and impact velocity play governing roles to trigger the onset of droplet rebound suppression. Here we present the role of impact velocity versus polymer concentration [refer to Fig. 7(a)], and it is clear that the critical velocity decreases with increasing polymer concentration. Impact velocity is the deciding factor behind the shear stress acting at the contact line during the onset of retraction of the droplet. The focus is put on the shear during the retraction phase as earlier reports have established that the spreading phase [5] is not altered by the elastic effects.

To emphasize the effect of viscoelasticity, we used a brine solution (aqueous NaCl) of viscosity almost similar to the high shear Newtonian viscosity value of the 2000 ppm PAAM solution. At the highest velocity of 2.5 m/s, the droplet of brine undergoes fragmentation into tiny droplets (very similar to water) showing no signs of rebound suppression (refer to Fig. 8). This signifies that the

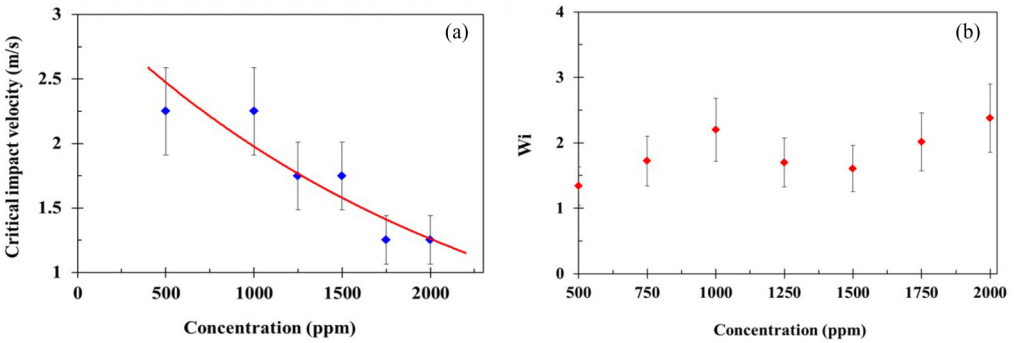


FIG. 7. (a) Critical impact velocity vs critical polymer concentration (ppm). The red line is a guide to the eye to emphasize the overall decreasing trend. (b) Critical Weissenberg number (Wi) vs polymer concentration (in ppm).

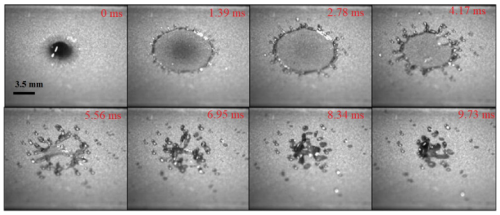


FIG. 8. Impact dynamics of salt water (viscosity ∼1.5 times of water, similar to the Newtonian viscosity of 2000 ppm PAAM solution). Images were taken at 1.39 ms intervals.

suppression of fragmentation and rebound is caused by the viscoelastic effect. Figure 8 shows the usual fragmentation observed in Newtonian solutions like Fig. 4 row (i) without any droplet rebound suppression (for the brine solutions). It is also noteworthy that the surface tension of the salt solution and polymer solution are very similar, and the static contact angles are also nearly equal. Hence the viscoelastic effects are responsible for the suppression of the fragmentation and rebound.

Experiments have revealed that for initiation of rebound suppression, there exist parallel criteria of critical impact velocity and critical polymer concentration. We propose that the product of shear rate $\dot{\gamma}$(localized to the vicinity of the contact line, at the instant of droplet retraction) and the viscoelastic relaxation time $\lambda$ of the polymer solutions, better known as the Weissenberg number ($\mathrm{Wi} = \lambda\,\dot{\gamma}$), is the driving entity behind this droplet suppression behavior. The shear rate during retraction was calculated as spreading dynamics was hardly affected due to polymers [1,4]. Shear rates were estimated by image analysis of the contact line during droplet retraction using ImageJ software. At the point of maximum spread and for a short time span during the onset retraction, the droplet assumes the shape of a flat disk [Fig. 3(a)]. The average thickness of the disc close to the contact line has been used as the vertical length scale to estimate shear rates. The typical shear rates at retraction of different impact velocity conditions have been tabulated in Table I. The critical shear rate for rebound suppression decreases with polymer concentration. In the shear rate estimation process, typically $10\%-15\%$ uncertainties have been noted between different repetition cases

With the increase of polymer concentration, the relaxation time will increase and is determined from the frequency-dependent viscoelastic moduli and the relaxation modulus using reported standard rheological analysis [26]. The viscoelastic moduli are determined at different dynamic conditions (using oscillatory frequency modulation at low strain amplitudes of ∼1%). The low strain amplitude is chosen as the dilute PAAM solutions used show linear viscoelastic response only up to ∼1% in the amplitude sweep rheology. The complex viscosity is determined from the frequency-dependent viscoelastic moduli, and effective relaxation times are deduced from standard methodology reported in the literature [26]. The typical relaxation timescales for the used PAAM

TABLE I. Relaxation times and the shear rate at retraction (for impact at the critical velocity) for different elastic fluid droplets.

| Polymer concentration (ppm) | Relaxation time (ms) | Critical impact velocity (ms) | Shear rate at retraction ($s^{-1}$) |
|---|---|---|---|
| 500 | 3.1 | 2.50 | 431.14 |
| 750 | 4.8 | 2.50 | 356.25 |
| 1000 | 6.5 | 2.25 | 334.90 |
| 1250 | 5.6 | 1.75 | 300.14 |
| 1500 | 4.7 | 1.75 | 337.90 |
| 1750 | 6.8 | 1.25 | 291.69 |
| 2000 | 9.1 | 1.25 | 263.30 |

solutions are tabulated in Table I. The associated uncertainties in determining relaxation timescales from the bulk rheological analysis may be up to 20%−50% [26].

For the relaxation timescales, agreement with reports on the viscoelastic behavior of PAAM solutions [27] was noted. Consequently, the impact velocity for which the rebound is arrested also decreases with the polymer concentration. This signifies that unlike proposed earlier, it will be possible to arrest rebound of droplets with vanishing amounts of polymer, if the impact velocity is sufficiently large (assuming that the infinitely dilute polymer solution can sustain the fragmentation due to high inertia impact, and the polymer dissolved has sufficiently long chains to ensure $\mathrm{Wi} > 1$ even at infinite dilution). Figure 7(b) shows the critical Wi versus polymer concentration. In spite of the uncertainties associated with the experimental materials and methodology, the Wi values can be observed to be confined within a narrow regime of $\sim 1.25-2.5$.

This scenario is identical to earlier studies where it was shown that for $\mathrm{Wi} > 1$ elastic instabilities sets in [28]. Although the present scenario does not lead to elastic turbulence [29] or elasto-inertial turbulence [30], suppression of non-Newtonian droplets rebound is clearly a viscoelastic phenomenon dependent on the critical value of Wi. High-precision experiments or numerical simulations may be used in future studies to identify a single unique value of Wi above which droplet rebound suppression will occur on SH surfaces. However, as all the values lie in $\mathrm{Wi} > 1$, it is confirmed that the elastic nature of the fluid plays a vital role in the arrest of the rebound behavior. The proposition of $\mathrm{Wi} > 1$ causing the onset of droplet rebound suppression is bolstered from the previous study [4] where they have reported that in all our experiments the relaxation time exceeds $1/\dot{\gamma}$ by at least one order of magnitude.

## IV. CONCLUSIONS

To conclude, in this work, we show the existence of parallel criteria of critical shear rate at retraction and polymer relaxation time on the onset of droplet rebound inhibition on SH surfaces. Previous studies focused on extensional viscosity [1], normal stresses [4], or stretching of polymer molecules at the receding contact line [5]. All these reasons are basically different manifestations of viscoelasticity, which is absent for Newtonian fluids. Our studies have shown that viscoelastic effects (primarily the relaxation timescale) are modified due to variation of polymer concentration and the shear rates during the retraction phase (which can be directly modulated by the impact height). Finally, we showed that the onset of droplet rebound suppression is observed for a critical threshold Weissenberg number.

The critical Wi is noted to be bound within a narrow regime for the spectrum of impact velocities and polymer concentrations studied. We believe that with experiments of higher precision (or intricate computations) a unique Wi value for properly characterized SH surfaces can be obtained, which triggers the onset of rebound inhibition. In addition, the temporal evolution of drops during retraction and rebound will be challenging phenomena for numerical simulations. Further, force measurement during impacts of non-Newtonian droplets can lead to greater insight [31]. Our studies may be beneficial in deciding the optimum amount of non-Newtonian additives and release height for maximizing the droplet depositions on hydrophobic substrates.

## ACKNOWLEDGMENTS

S.R.M. would like to thank the Ministry of Human Resource Development, Government of India, for a scholarship. D.S. and P.D. would like to thank IIT Ropar for funding the present work (Grants No. 9-246/2016/IITRPR/144 and No. IITRPR/Research/193, respectively). We thank the anonymous reviewers for their inputs, which have helped towards improving the readability of the article.

[1] V. Bergeron, D. Bonn, J. Y. Martin, and L. Vovelle, Controlling droplet deposition with polymer additives, Nature (London) **405**, 772 (2000).
[2] R. Crooks, J. Cooper-Whitez, and D. V. Boger, The role of dynamic surface tension and elasticity on the dynamics of drop impact, Chem. Eng. Sci. **56**, 5575 (2001).
[3] A. Rozhkov, B. Prunet-Foch, and M. Vignes-Alder, Impact of drops of polymer solutions on small targets, Phys. Fluids **15**, 2006 (2003).
[4] D. Bartolo, A. Boudaoud, G. Narcy, and D. Bonn, Dynamics of Non-Newtonian Droplets, Phys. Rev. Lett. **99**, 174502 (2007).
[5] M. I. Smith and V. Bertola, Effect of Polymer Additives on the Wetting of Impacting Droplets, Phys. Rev. Lett. **104**, 154502, (2010).
[6] J. Han and C. Kim, Spreading of Boger fluid on horizontal surface, J. Non-Newtonian Fluid Mech. **202**, 1202013.
[7] D. Zang, X. Wang, X. Geng, Y. Zhang, and Y. Chen, Impact dynamics of droplets with silica nanoparticles and polymer additives, Soft Matter **9**, 394 (2013).
[8] N. Mourougou-Candoni, B. Prunet-Foch, F. Legay, M. Vignes-Adler, and K. Wong, Influence of dynamic surface tension on the spreading of surfactant solution droplets impacting onto a low-surface energy solid substrate, J. Colloid Interface Sci. **192**, 129 (1997).
[9] S. Yun, J. Hong, and K. H. Kang, Suppressing drop rebound by electrically driven shape distortion, Phys. Rev. E **87**, 033010, (2013).
[10] S. Yun and G. Lim, Ellipsoidal drop impact on a solid surface for rebound suppression, J. Fluid Mech. **752**, 266 (2014).
[11] M. Gumemas, A. G. Marın, and D. Lohse, Drop impact experiments of non-Newtonian liquids on micro-structured surfaces, Soft Matter **8**, 10725 (2012).
[12] L. H. Luu and Y. Forterre, Drop impact of yield stress fluids, J. Fluid Mech. **632**, 301 (2009).
[13] F. Boyer, E. S. Nava, J. H. Snoeijer, J. F. Dijksman, and D. Lohse, Drop impact of shear thickening fluids, Phys. Rev. Fluids **1**, 013901 (2016).
[14] N. Sahoo, G. Khurana, A. R. Harikrishnan, D. Samanta, and P. Dhar, Interplay of substrate inclination and wettability on droplet impact dynamics, Euro. J. Mech. - B/Fluids **79**, 27 (2020).
[15] P. P. Bhatt, S. Appathurai, M. T. Harris, M. Pasquali, G. H. McKinley, and O. A. Basaran, Formation of beads-on-a-string structures during break-up of viscoelastic filaments, Nat. Phys. **6**, 625 (2010).
[16] B. Keshavaraj, E. C. Houze, J. R. Moore, M. R. Korener, and G. H. McKinley, Ligament Mediated Fragmentation of Viscoelastic Liquids, Phys. Rev. Lett. **117**, 154502 (2016).
[17] C. M. White and G. Mungal, Mechanics and prediction of turbulent drag reduction with polymer additives, Ann. Rev. Fluid Mech. **40**, 235 (2008).
[18] C. Wagner, Y. Amarouchene, D. Bonn, and J. Eggers, Droplet Detachment and Satellite Bead Formation in Viscoelastic Fluids, Phys. Rev. Lett. **95**, 164504 (2005).
[19] R. Sattler, C. Wagner, and J. Eggers, Blistering Pattern and Formation of Nanofibers in Capillary Thinning of Polymer Solutions, Phys. Rev. Lett. **100**, 164502 (2008).
[20] M. S. N. Olivera, R. Yeh, and G. H. McKinley, Iterated stretching, extensional rheology and formation of beads-on-a- string structures in polymer solutions, J. Non-Newtonian Fluid Mech. **137**, 137 (2006).
[21] See Supplemental Material at http://link.aps.org/supplemental/10.1103/PhysRevFluids.4.103303 for details on filament longevity, retraction behavior of the droplets, and physical structure of the superhydrophobic surfaces.
[22] C. E. Clavijo, J. Crockett, and D. Maynes, Wenzel to Cassie transition during droplet impingement on a superhydrophobic surface, Phys. Rev. Fluids **1**, 073902 (2016).
[23] C. Lee, Y. Nam, H. Lastakowski, J. I. Hur, S. Shin, A.-L. Biance, C. Pirat, C.-J. "CJ" Kim, and C. Ybert, Two types of Cassie-to-Wenzel wetting transitions on superhydrophobic surfaces during drop impact, Soft Matter **11**, 4592 (2015).
[24] C. Antonini, F. Villa, I. Bernagozzi, A. Amirfazli, and M. Marengo, Drop rebound after impact: The role of the receding contact angle, Langmuir **29**, 16045 (2013).
[25] K. Murugaddos, P. Dhar, and S. Das, Role and significance of wetting pressures during droplet impact on structured superhydrophobic surfaces, Eur. Phys. J. E **40**, 1 (2017).

[26] K. S. Wissbrun and A. C. Griffin, Rheology of a thermotropic polyester in the nematic and isotropic states, J. Polymer Sci.: Polymer Phys. **20**, 1835 (1982).
[27] D. Samanta, Ph.D. thesis, University of Saarbruecken, Germany, 2012.
[28] A. N. Morozov and W. V. Sarloos, An introductory essay on subcritical instabilities and the transition to turbulence in viscoelastic parallel shear flows, Phys. Rep. **447**, 112 (2007).
[29] A. Groisman and V. Steinberg, Elastic turbulence in a polymer solution flow, Nature (London) **405**, 53 (2000).
[30] D. Samanta, Y. Dubief, M. Holzner, C. Schafer, A. N. Morozov, C. Wagner, and B. Hof, Elasto-inertial turbulence, Proc. Natl Acad. Sci. USA **110**, 10557 (2013).
[31] L. Gordillo, T. P. Sung, and X. Cheng, Dynamics of drop impact on solid surfaces: Evolution of impact force and self-similar profiles, J. Fluid Mech. **840**, 190 (2018).